

Are your **MRI contrast agents** cost-effective?

Learn more about generic **Gadolinium-Based Contrast Agents**.



**FRESENIUS
KABI**

caring for life

AJNR

Human Brain Hemorrhage: Quantification of Perihematoma Edema by Use of Diffusion-Weighted MR Imaging

J. Ricardo Carhuapoma, Peter B. Barker, Daniel F. Hanley, Paul Wang and Norman J. Beauchamp

This information is current as of April 17, 2024.

AJNR Am J Neuroradiol 2002, 23 (8) 1322-1326
<http://www.ajnr.org/content/23/8/1322>

Human Brain Hemorrhage: Quantification of Perihematoma Edema by Use of Diffusion-Weighted MR Imaging

J. Ricardo Carhuapoma, Peter B. Barker, Daniel F. Hanley,
Paul Wang, and Norman J. Beauchamp

BACKGROUND AND PURPOSE: Animal models have clearly shown a critical role for extravascular blood in the initiation of the vasogenic edema associated with intracerebral hemorrhage (ICH). Nevertheless, the relevance of these observations to the human disease process has not been evaluated. With a prospectively collected cohort of nine patients, we report the relation between intraparenchymal blood clot volume and elevation of perihematoma brain tissue (and homologous contralateral brain tissue) apparent diffusion coefficient (ADC).

METHODS: Patients with acute and subacute supratentorial ICH were prospectively evaluated by using diffusion-weighted imaging. ADC was measured in perihematoma tissue and in homologous contralateral regions. The relationship between ADC and volume of hematoma was determined by using linear regression analysis.

RESULTS: Nine patients were enrolled in the study. The mean hematoma volume was 30.8 cc (range, 2.6–74 cc). The ADC in the perihematoma regions was $172.5 \times 10^{-5} \text{ mm}^2/\text{s}$ (range, $120.1\text{--}302.5 \times 10^{-5} \text{ mm}^2/\text{s}$) and in the contralateral corresponding regions of interest was $87.6 \times 10^{-5} \text{ mm}^2/\text{s}$ (range, $76.5\text{--}102.1 \times 10^{-5} \text{ mm}^2/\text{s}$) ($P = .02$). The Pearson correlation coefficient for the ADC in surrounding edema and hematoma volume was 0.7 ($P = .04$). The correlation coefficient between hematoma volume and contralateral hemisphere ADC was 0.8 ($P = .02$).

CONCLUSION: We report a significant direct correlation between ICH volume and degree of ADC elevation in perihematoma and ADC values in contralateral corresponding brain tissue. These findings suggest a dose-effect interaction between volume and concentration of blood products and intensity of response that brain tissue exhibits in blood-mediated edema. Prospective natural history and interventional studies are required to confirm this biologically meaningful correlation in patients with ICH.

Intracerebral hemorrhage (ICH) is associated with significant morbidity and mortality (1). Several processes contribute to this problem, the most obvious

being hematoma enlargement and the development of perihematoma brain edema. After ICH, serum protein penetration from the clot into the surrounding white matter, followed by blood-brain barrier breakdown due to inflammation, have been proposed as mechanisms leading to edema formation in the extracellular compartment (2–4). This edema fluid, evident on CT scans (hypoattenuated halo) and MR images (T2 hyperintense halo), can exceed the original hematoma volume by a factor of two and may therefore account for the neurologic deterioration observed during the acute and subacute stages of the disease (5, 6).

Treatment options for the mass effect induced by the hematoma and surrounding edema include the surgical evacuation and decompression of the hematoma and medical management and critical care if elevated intracranial pressure (ICP) is identified (7). However, specific treatments capable of modifying

Received November 21, 2001; accepted April 3, 2002.

Presented in part as an abstract at the 26th American Heart Association International Stroke Meeting, Fort Lauderdale, 2000.

Supported in part by the Daland Fellowship for Clinical Research Award from the American Philosophical Society (to J.R.C.) and by a grant from the American Roentgen Ray Society (to N.J.B.).

From the Neurosciences Critical Care and Stroke Program (J.R.C.), Wayne State University School of Medicine, Detroit, MI, and the Divisions of Neurosciences Critical Care (D.F.H.) and Neuroradiology (P.B.B., P.W., N.J.B.), The Johns Hopkins Medical Institutions, Baltimore, MD.

Address reprint requests to J. Ricardo Carhuapoma, MD, Wayne State University, Department of Neurology, University Health Center 8C-25, 4201 St. Antoine Boulevard, Detroit, MI 48201.

© American Society of Neuroradiology

the natural history of the disease are lacking. An improved understanding of the pathophysiological processes that participate in secondary neuronal damage after ICH is required to intelligently design and conduct therapeutic research in this field.

Diffusion-weighted imaging has already proved valuable in diagnosing and studying the natural history of ischemic stroke by helping in early definition of deeply ischemic or infarcted brain tissue (8, 9). Nevertheless, diffusion-weighted imaging has only recently been recognized as a useful tool in the study of perihematoma tissue perfusion and metabolism in patients with ICH (10, 11). In a previous report, the feasibility of diffusion-weighted imaging and proton MR spectroscopic imaging in the study of perihematoma edema and metabolism was described. The results of that report were consistent with increased perihematoma tissue water content defined as elevated apparent diffusion coefficient (ADC) values relative to contralateral, homologous brain regions, presumably due mainly to vasogenic edema (11). To test the hypothesis that there is a dose-effect relationship between blood clot volume and tissue water content as an indirect measure of severity of blood-brain barrier breakdown and vasogenic brain edema formation, we analyzed the interaction between the volume of ICH and the magnitude of ADC changes in the surrounding perihematoma edema and in contralateral brain tissue by using diffusion-weighted imaging in a pilot cohort of patients with ICH.

Methods

Patients

With approval from our institution's investigational review board and after obtaining informed consent, consecutive patients with diagnoses of acute and subacute spontaneous supratentorial ICH were screened and enrolled in this pilot study if they had new neurologic deficits and findings of CT of the head that were compatible with supratentorial ICH. Contraindications for MR imaging, allergy to contrast material, and ICH secondary to known anticoagulation or abnormal prothrombin or partial thromboplastin time were considered exclusion criteria. Women of childbearing age were screened for pregnancy before being considered candidates for the study. The MR imaging studies were performed only after patients were deemed clinically stable to be safely transported to the MR imaging facility.

MR Imaging Techniques

The studies were performed on a 1.5-T General Electric imager with quadrature head coil. The following MR images were recorded: 1) sagittal view T1-weighted localizer images; 2) axial view spin-echo spin attenuation and T2-weighted images; and 3) diffusion-weighted echo-planar images. All sequences (except sequence 1) were recorded in an oblique-axial plane, parallel to the anterior commissure-posterior commissure line, at the same section locations, and with the same section thickness (5 mm).

Conventional MR Imaging.—Sagittal view T1-weighted and axial view T2-weighted images were recorded with standard spin-echo sequences. For T1-weighted images, the acquisition parameters were as follows: field of view, 24 mm; section thickness, 5 mm; section gap, 1 mm; 535/10/1 (TR/TE/number of excitations); matrix, 256 × 192. For T2-weighted images, the

acquisition parameters were as follows: field of view, 24 mm; section thickness, 5 mm; 3000/30, 100/0.75; matrix, 256 × 192; flow compensation; and variable bandwidth.

Diffusion-Weighted Echo-Planar Imaging.—Multi-section, single shot, diffusion-weighted echo-planar imaging of the whole brain was performed. The following parameters were used: field of view, 24 mm; section thickness, 5 mm; 4000/100/1; matrix, 128 × 128; diffusion time, 40 ms; and diffusion gradient length, 25 ms. Diffusion gradient strengths of 0.1, 1.1, 1.5, 1.9, and 2.2 G/cm were used, giving b values of 2, 216.5, 433, 649.5, and 866 mm²/s, respectively, applied sequentially in the x, y, and z gradient directions. Isotropic diffusion-weighted images and images of the ADC were reconstructed:

$$ADC = (D_{xx} + D_{yy} + D_{zz})/3$$

Diffusion Image Analysis

Quantitative image analysis was performed on a Dell computer by using the Scion Image for Windows program, a personal computer version of NIH Image (version 1.61; Wayne Rasband, National Institutes of Health, Bethesda, MD). Feasibility of assessment was based on ability to obtain diffusion data in perihematoma brain regions. Images were evaluated for the presence of obscuration secondary to susceptibility artifact. The hematoma was visualized on conventional T2-weighted MR images in all cases; all cases also exhibited T2 hyperintensity in brain parenchyma surrounding the hematoma. The T2 hyperintense rim was outlined on the low b-value diffusion-weighted echo-planar images manually by two investigators (J.R.C., P.B.B.). The low b-value diffusion-weighted echo-planar images are essentially T2-weighted images with the same section locations and spatial distortions as the high b-value diffusion-weighted echo-planar images. The coordinates of these regions of interest were then transferred to the calculated ADC images for measurement of hematoma and perihematoma diffusion coefficients. After visual identification, ADC was also measured in similar regions of interest in the contralateral hemisphere. ADC images were also screened by two investigators (J.R.C., P.B.B.) for focal abnormalities beyond the regions identified on the T2-weighted MR images.

Measurement of Hematoma Volume

Using the Scion Image for Windows program, volume measurements of blood clots were obtained according to their specific signal intensity on T2-weighted MR images. On the basis of these signal intensity properties, the boundaries of the hematoma areas were traced by hand on each section. The cross-sectional area of each section was then multiplied by the section thickness and summed to produce the total hematoma volume.

Statistical Method

SPSS (version 10.1; SPSS Inc., Chicago, IL) was used for data analysis. A paired *t* test was used to determine whether there was a significant difference in ADC values between perihematoma and corresponding contralateral brain areas, and a 95% confidence interval was calculated for the mean difference. To determine the presence or absence of a correlation between variables, Pearson correlation was used, accepting statistical significance only if *P* < .05.

Results

Between August 1997 and December 1999, nine consecutive patients who met all the inclusion criteria were enrolled in this pilot study.

Clinical and radiologic features of patient cohort

Patient (No.)	Age (y)/ Sex	MAP (mm Hg)	Time to MR Imaging (days)	Cause of ICH	Location	Hematoma Volume (cc) on T2-weighted MR Images	ADC in Perihematoma Edema ($\times 10^{-5}$ mm ² /s)	ADC in Contralateral Hemisphere ($\times 10^{-5}$ mm ² /s)
1	62/M	120	2	HTN	L thalamus + IVH	2.6	120.1 \pm 22.6	92.7 \pm 21
2	72/M	95	2	HTN	L basal ganglia	6.5	131.7 \pm 1.9	76.5 \pm 1.3
3	44/F	85	3	Probable AVM	R temporal lobe	32	137.2 \pm 16.5	86.2 \pm 7
4	87/F	105	4	HTN	L basal ganglia	37	162.0 \pm 14.9	88.9 \pm 4.2
5	52/F	130	2	HTN	L basal ganglia	26	223.1 \pm 42.1	84.9 \pm 6.7
6	70/M	95	6	HTN	L basal ganglia	74	302.5 \pm 46.5	102.1 \pm 8.7
7	36/M	90	2	Cocaine induced	R parietal + IVH	39	194.7 \pm 51.9	86.7 \pm 11.9
8	61/M	110	1	HTN	L basal ganglia	4.4	140.8 \pm 12.8	77.7 \pm 0.4
9	87/F	90	9	Probable AA	L basal ganglia + IVH	56	140.6 \pm 14.8	92.5 \pm 14.2

Note.—MAP indicates mean arterial pressure; ICH, intracerebral hemorrhage; ADC, apparent diffusion coefficient; M, male; F, female; HTN, hypertension; AVM, arteriovenous malformation; AA, amyloid angiopathy; IVH, intraventricular hemorrhage.

Demographic Characteristics

The mean age of the study cohort was 63.4 years (range, 36–87 years; SD \pm 17.7 years), and the male to female ratio was 5:4. The mean time from symptom onset to initial MR imaging was 3.4 days (range, 1–9 days; SD \pm 2.6 days) for all nine patients.

Clinical Features

No blood pressure or ventilatory manipulation was performed immediately before or during the MR imaging studies (Table 1). The cause of ICH was systemic hypertension in six patients, probable vascular malformation in one patient, probable amyloid angiopathy in one patient, and cocaine use in one patient. The hematoma was located in the basal ganglia or thalamus in seven patients and in the lobar area in two. Two patients each had an intraventricular hemorrhage component. The mean arterial pressure in the study cohort at the time of the first MR imaging study was 102.2 mm Hg (range, 85–130 mm Hg; SD \pm 15.2 mm Hg).

Radiologic Features

The mean hematoma volume was 30.8 cm³ (range, 2.6–74 cm³; SD \pm 24.3 cm³), as measured on initial MR images of the brain. High signal intensity on T2-weighted MR images was found predominantly in the white matter surrounding the hematoma in every patient studied (Fig 1). Elevated ADC values (relative to homologous brain regions in the contralateral hemisphere) matching areas of high T2 signal intensity were found surrounding the hematoma in every patient, with mean ADC values of 172.5×10^{-5} mm²/s (range, $120.1\text{--}302.5 \times 10^{-5}$ mm²/s; SD \pm 58.9×10^{-5} mm²/s) and 87.6×10^{-5} mm²/s (range, $76.5\text{--}102.1 \times 10^{-5}$ mm²/s; SD \pm 7.9×10^{-5} mm²/s) in ipsi- and contralateral regions of interest, respectively. Using a paired *t* test, the obtained *t* statistic and *P* value were 4.7 and 0.02, respectively. The 95% confidence interval for the mean difference was 42.8 to 127. Patient 6 showed an area of reduced ADC superior to the

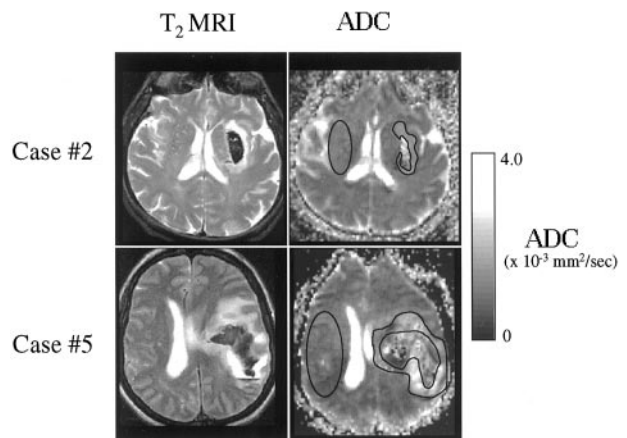


Fig 1. MR images of two patients with ICH show the presence of a hyperintense halo on T2-weighted MR images (*T*₂ MRI) and elevated ADC values in corresponding brain regions on diffusion-weighted images. Both characteristics are compatible with elevated interstitial tissue water content, suggestive of vasogenic brain edema. The diffusion-weighted images show regions of interest in the perihematoma tissue and in the contralateral hemisphere that were chosen for ADC analysis.

blood clot ($51.5 \pm 8.9 \times 10^{-5}$ mm²/s), with corresponding normal T2 signal intensity, consistent with acute cerebral ischemia, in addition to perihematoma T2 signal intensity.

For perihematoma edema regions, a direct correlation between ADC and hematoma volume was observed, with a Pearson correlation coefficient of 0.7 and *P* = .04 (Fig 2). When ADC values in homologous brain regions in the contralateral, noninjured hemisphere were analyzed, the degree of correlation with the ICH volume was 0.8 and *P* = .02 (Fig 3).

Because of the known progression of vasogenic edema over time, we investigated the relation of hematoma age and ADC values in brain tissue. There was no significant correlation between hematoma age and perihematoma (Pearson correlation coefficient 0.2 and *P* = .6) or contralateral (Person correlation coefficient 0.6 and *P* = .06) ADC regions of interest in our patient cohort.

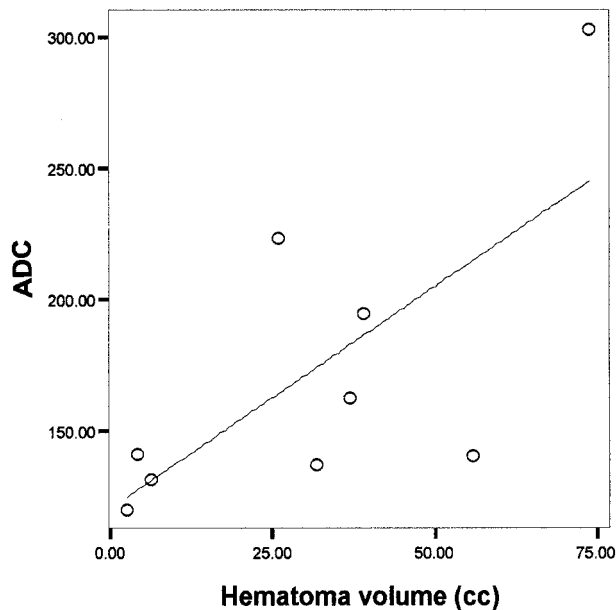


FIG 2. Significant correlation between blood clot volume and ADC in the perihematoma tissue surrounding edema in nine patients with ICH (Pearson correlation coefficient 0.7, $P = .04$).

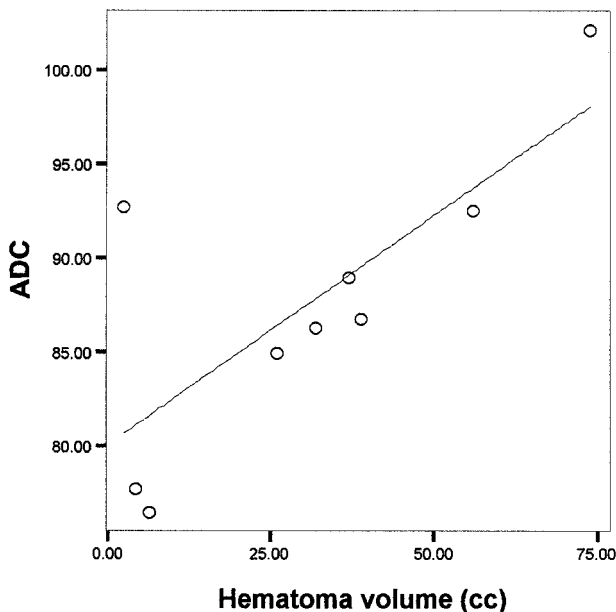


FIG 3. Significant correlation between blood clot volume and ADC in corresponding homologous brain regions contralateral to the high T2 signal intensity perihematoma halo used as surrogate of vasogenic brain edema in nine patients with ICH (Pearson correlation coefficient 0.8, $P = .02$).

Discussion

We report a significant direct relationship between ADC elevation in areas of perihematoma brain edema and volume of hematoma in nine patients with ICH. Furthermore, a significant correlation was also observed in contralateral brain tissue between ADC value and ICH volume. Although a number of factors can affect the ADC values surrounding the ICH, in the current patient group, we interpreted the ADC elevation to be indirect evidence of vasogenic edema.

Although it may seem axiomatic to expect larger edema volumes and water content in patients with large intraparenchymal hematomas, the current study represents a first attempt to *indirectly quantify in vivo the intensity of vasogenic brain edema* in response to blood and its degradation products after human ICH. We postulate that this observed correlation may represent a dose-effect relationship between the concentration of blood components or their degradation products and the severity of blood-brain barrier disruption with the formation of vasogenic edema surrounding the hematoma. The ADC values observed in the contralateral hemisphere may represent a graded response of neuronal tissue to remote "toxic" effects induced by blood or its degradation products. Competing hypotheses to explain this novel observation are the global effects of elevated ICP and diaschisis. Although only one patient (patient 7) required external ventricular drainage for treatment of obstructive hydrocephalus and for ICP monitoring, the remaining patients did not exhibit clinical evidence of significantly elevated ICP to justify the placement of an ICP monitor. Furthermore, because severely elevated ICP induces a state of ischemic encephalopathy, ADC values would be expected to be consistent with early cytotoxic brain edema as opposed to what was observed in our group of patients. If diaschisis plays a role in the observed ADC, response of neuronal tissue contralateral to the hematoma remains to be determined because MR imaging research in this pathophysiological state is lacking.

The nature and progression of perihematoma cerebral edema has received significant attention during the last decade. Several animal models have been used for this purpose, including a rodent model of autologous blood inoculation in the striatum. Several lines of evidence seem to suggest that blood, and more specifically thrombin, plays a central role in the genesis of perihematoma edema after ICH (12–15). Initial clot retraction and then passage of serum proteins from the clot mass to the perihematoma extracellular compartment may account for the initial increment in surrounding tissue water content (4). However, clear inflammatory mechanisms are well developed after 3 days from initial injury, as reported by Gong et al (2). Xi et al (16) showed that thrombin is central in the induction of direct neurotoxicity and in the generation of blood-brain barrier disruption and the accumulation of extracellular water near the hematoma in a dose-response manner. Recently, the same group of investigators proposed that preconditioning with thrombin can ameliorate the subsequent development of vasogenic edema after the induction of ICH in rodents, the effect apparently mediated by heat-shock protein induction after a first exposure of brain tissue to thrombin.

Several attempts to elucidate best therapies for ICH victims have been unsuccessful for several reasons. Medical treatments are, for the most part, non-specific. Their main target is the treatment of elevated ICP and the delivery of general critical care to neurologically debilitated patients. Hematoma evac-

uation (surgically or by aspiration), on the other hand, has an undefined role for the vast majority of patients with ICH (17–22). Thus far, preliminary clinical experience obtained from small series of patients by using stereotactic aspiration of cerebral hematomas suggests that this technique is safe and is capable of improving neurologic outcome when compared with historical controls. The mechanism(s) of improved outcome could be the prevention of hematoma enlargement but also the arrest or amelioration of the development of perihematoma edema, which could reach 200% of the initial hematoma mass (5). Recently, Wagner et al (23), by using a porcine model of ICH, showed that aspiration of the blood clot reduced mass effect and the development of vasogenic edema and improved neurologic outcome. Altumbabic et al (24) achieved similar results in a rodent model of ICH. Therefore, it seems reasonable that vasogenic edema could serve as a therapeutic target of medical or more invasive interventions targeted to the triggering event, the ICH, or the development of subsequent surrounding edema.

The small size of the patient cohort reported herein, in addition to the variable times (2–9 days) when the MR imaging studies were performed, clearly prevent us from arriving at generalized conclusions. However, we are able to report a direct correlation between the ICH volume and the degree of ADC elevation in perihematoma brain edema regions and in contralateral brain tissue, as compared with normative values obtained in healthy persons, as reported by Uluğ and van Zijl (25). These correlations should be considered hypothesis-generating only at this stage. Nevertheless, if confirmed in a larger, prospective study, this dose-effect relationship between volume and concentration of blood components and the subsequent diffuse response of neuronal tissue to injury could allow diffusion-weighted imaging to become a powerful research tool capable of doing the following: 1) quantifying in vivo the biologic effects of ICH on neuronal tissue, 2) improving our knowledge of the natural progression of perihematoma vasogenic brain edema, 3) assessing the future impact of vasogenic brain edema and elevated brain water content on neurocognitive outcome after ICH, and 4) assessing effects of future treatments aimed to block these nonischemic mechanisms of neuronal injury.

Acknowledgments

We thank Drs. Aziz Uluğ and Peter van Zijl for the diffusion-weighted imaging sequence.

References

- Broderick J, Brott T, Tomsick T, Tew J, Duldner J, Huster G. Management of intracerebral hemorrhage in a large metropolitan population. *Neurosurgery* 1994;34:882–887
- Gong C, Hoff JT, Keep RF. Acute inflammatory reaction following experimental intracerebral hemorrhage in rat. *Brain Res* 2000;871:57–65
- Xi G, Wagner KR, Keep RF, et al. Role of blood clot formation on early edema development after experimental intracerebral hemorrhage. *Stroke* 1998;29:2580–2586
- Wagner KR, Xi G, Hua Y, et al. Lobar intracerebral hemorrhage model in pigs: rapid edema development in perihematoma white matter. *Stroke* 1996;27:490–497
- Carhuapoma JR, Beauchamp NJ. Brain edema after intracerebral hemorrhage: a magnetic resonance imaging volumetric analysis. *Neurology* 2000;54[suppl 7]:A375–A376
- Zazulia AR, Diringer MN, Derdeyn CP, Powers WJ. Progression of mass effect after intracerebral hemorrhage. *Stroke* 1999;30:1167–1173
- Broderick JP, Adams HP Jr, Barsan W, et al. Guidelines for the management of spontaneous intracerebral hemorrhage: a statement for healthcare professionals from a special writing group of the Stroke Council, American Heart Association. *Stroke* 1999;30:905–915
- Beauchamp NJ, Bryan RN. Acute cerebral ischemic infarction: a pathophysiologic review and radiologic perspective. *AJR Am J Roentgenol* 1998;171:73–84
- Uluğ AM, Beauchamp N Jr, Bryan RN, van Zijl PC. Absolute quantitation of diffusion constants in human stroke. *Stroke* 1997;28:483–90
- Kidwell CS, Saver JL, Mattiello J, et al. Diffusion-perfusion MR evaluation of perihematoma injury in hyperacute intracerebral hemorrhage. *Neurology* 2001;57:1611–1617
- Carhuapoma JR, Wang PY, Beauchamp NJ, Keyl PM, Hanley DF, Barker PB. Diffusion-weighted MR imaging and proton MR spectroscopic imaging in the study of secondary neuronal injury after intracerebral hemorrhage. *Stroke* 2000;31:726–732
- Lee KR, Betz AL, Keep RF, Chenevert TL, Kim S, Hoff JT. Intracerebral infusion of thrombin as a cause of brain edema. *J Neurosurg* 1995;83:1045–1050
- Lee KR, Betz AL, Kim S, Keep RF, Hoff JT. The role of the coagulation cascade in brain edema formation after intracerebral hemorrhage. *Acta Neurochir (Wien)* 1996;138:396–400
- Lee KR, Colon GP, Betz AL, Keep RF, Kim S, Hoff JT. Edema from intracerebral hemorrhage: the role of thrombin. *J Neurosurg* 1996;84:91–96
- Lee KR, Kawai N, Kim S, Sagher O, Hoff JT. Mechanisms of edema formation after intracerebral hemorrhage: effects of thrombin on cerebral blood flow, blood-brain barrier permeability, and cell survival in a rat model. *J Neurosurg* 1997;86:272–278
- Xi G, Keep RF, Hua Y, Xiang J, Hoff JT. Attenuation of thrombin-induced brain edema by cerebral thrombin preconditioning. *Stroke* 1999;30:1247–1255
- Batjer HH, Reisch JS, Allen BC, Plaizier LJ, Su CJ. Failure of surgery to improve outcome in hypertensive putaminal hemorrhage: a prospective randomized trial. *Arch Neurol* 1990;47:1103–1106
- Fayad PB, Awad IA. Surgery for intracerebral hemorrhage. *Neurology* 1998;51:S69–S73
- Hankey GJ, Hon C. Surgery for primary intracerebral hemorrhage: is it safe and effective? a systematic review of case series and randomized trials. *Stroke* 1997;28:2126–2132
- Morgenstern LB, Frankowski RF, Shedden P, Pasteur W, Grotta JC. Surgical treatment for intracerebral hemorrhage (STICH): a single-center, randomized clinical trial. *Neurology* 1998;51:1359–1363
- Schwarz S, Jauss M, Krieger D, Dorfler A, Albert F, Hacke W. Haematoma evacuation does not improve outcome in spontaneous supratentorial intracerebral haemorrhage: a case-control study. *Acta Neurochir (Wien)* 1997;139:897–903
- Zuccarello M, Brott T, Derex L, et al. Early surgical treatment for supratentorial intracerebral hemorrhage: a randomized feasibility study. *Stroke* 1999;30:1833–1839
- Wagner KR, Xi G, Hua Y, et al. Ultra-early clot aspiration after lysis with tissue plasminogen activator in a porcine model of intracerebral hemorrhage: edema reduction and blood-brain barrier protection. *J Neurosurg* 1999;90:491–498
- Altumbabic M, Peeling J, Del Bigio MR. Intracerebral hemorrhage in the rat: effects of hematoma aspiration. *Stroke* 1998;29:1917–1922
- Uluğ AM, van Zijl PC. Orientation-independent diffusion imaging without tensor diagonalization: anisotropy definitions based on physical attributes of the diffusion ellipsoid. *J Magn Reson Imaging* 9:804–813, 1999.